International Journal of Nanomedicine

Dovepress
open access to scientific and medical research

Open Access Full Text Article

ORIGINAL RESEARCH

Intranasal Delivery of Endothelial Cell-Derived Extracellular Vesicles with Supramolecular Gel Attenuates Myocardial Ischemia-Reperfusion Injury

Junzhuo Wang[1,*], Ying Tan[1,*], Yang Dai[2,3,*], Ke Hu[2], Xi Tan[1], Shaoli Jiang[4], Guannan Li[1], Xinlin Zhang[1], Lina Kang[1], Xiaojian Wang[4], Biao Xu[1,2]

[1]Department of Cardiology, Nanjing Drum Tower Hospital, Affiliated Hospital of Nanjing University Medical School, Nanjing, People's Republic of China; [2]Department of Cardiology, Nanjing Drum Tower Hospital, Clinical College of Nanjing Medical University, Nanjing, People's Republic of China; [3]Department of Geriatrics, Nanjing Drum Tower Hospital, Affiliated Hospital of Nanjing University Medical School, Nanjing, People's Republic of China; [4]Institute of Advanced Synthesis, School of Chemistry and Molecular Engineering, Nanjing Tech University, Nanjing, People's Republic of China

*These authors contributed equally to this work

Correspondence: Biao Xu, Department of Cardiology, the Affiliated Hospital of Nanjing University Medical School, No. 321 Zhongshan Road, Nanjing, Jiangsu, People's Republic of China, Email xubiao62@nju.edu.cn; Xiaojian Wang, Institute of Advanced Synthesis, School of Chemistry and Molecular Engineering, Nanjing Tech University, Nanjing, People's Republic of China, Email ias_xjwang@njtech.edu.cn

Purpose: Myocardial ischemia-reperfusion injury after myocardial infarction has always been a difficult problem in clinical practice. Endothelial cells and their secreted extracellular vesicles are closely related to inflammation, thrombosis formation, and other processes after injury. Meanwhile, low-molecular-weight gelators have shown great potential for nasal administration. This study aims to explore the therapeutic effects and significance of endothelial cell-derived extracellular vesicles combined with a hydrogel for nasal administration on myocardial ischemia-reperfusion injury.

Methods: We chose a gel system composed of a derivative of glutamine amide and benzaldehyde as the extracellular vesicle delivery vehicle. This hydrogel was combined with extracellular vesicles extracted from mouse aortic endothelial cells and administered multiple times intranasally in a mouse model of ischemia-reperfusion injury to the heart. The delivery efficiency of the extracellular vesicle-hydrogel combination was evaluated by flow cytometry and immunofluorescence. Echocardiography, TTC Evan's Blue and Masson's staining were used to assess mouse cardiac function, infarct area, and cardiac fibrosis level. Flow cytometry, ELISA, and immunofluorescence staining were used to investigate changes in mouse inflammatory cells, cytokines, and vascular neogenesis.

Results: The vesicles combined with the hydrogel have good absorption in the nasal cavity. The hydrogel combined with vesicles reduces the levels of pro-inflammatory Ly6C (high) monocytes/macrophages and neutrophils. It can also reduce the formation of microcirculation thrombi in the infarcted area, improve endothelial barrier function, and increase microvascular density in the injured area. As a result, the heart function of mice is improved and the infarct area is reduced.

Conclusion: We first demonstrated that the combination of extracellular vesicles and hydrogel has a better absorption efficiency in the nasal cavity, which can improve myocardial ischemia-reperfusion injury by inhibiting inflammatory reactions and protecting endothelial function. Nasal administration of vesicles combined with hydrogel is a potential therapeutic direction.

Keywords: myocardial ischemia-reperfusion injury, extracellular vesicles, hydrogel, intranasal delivery, inflammation

Introduction

Myocardial infarction is a leading cause of death and disability worldwide.[1] Currently, the most important treatments to restore coronary blood flow are cutaneous coronary intervention and fibrinolytic drug reperfusion therapy. However, these treatments can lead to cardiomyocyte dysfunction and worsen tissue damage, a process known as myocardial ischemia-reperfusion (IR) injury. Unfortunately, there is currently no effective treatment for this type of injury.[2,3]

Received: 23 May 2023
Accepted: 12 September 2023
Published: 27 September 2023

Graphical Abstract

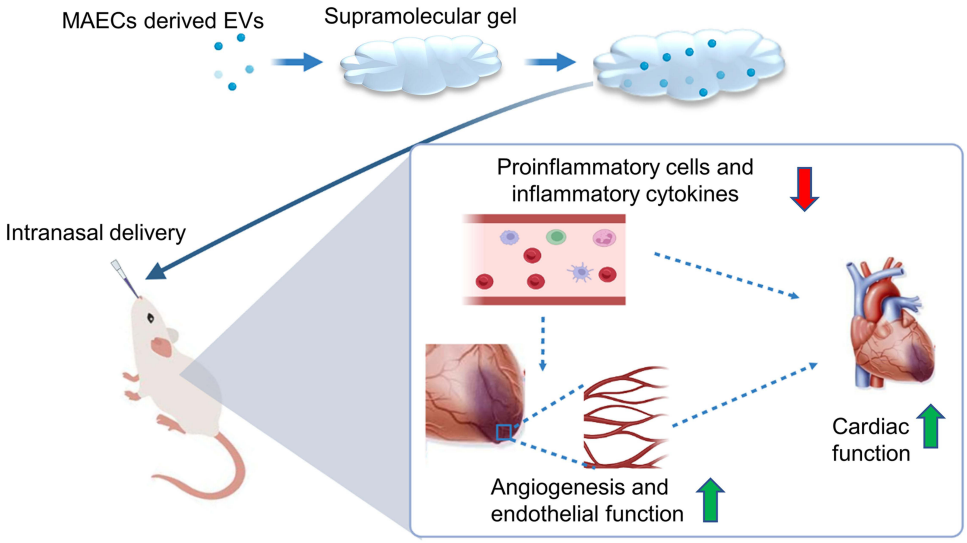

Therefore, it is crucial to explore therapeutic strategies for cardiac IR injury. During cardiac ischemia, the barrier function of vascular endothelial cells is impaired, leading to increased permeability and significant infiltration of immune cells.[4] During the process of reperfusion, the sudden reoxygenation, generation of reactive oxygen species, and activation of the complement pathway can further increase tissue damage.[5] Necrotic and stressed/damaged cells, along with damaged extracellular matrix, release damage-associated molecular patterns (DAMPs). DAMPs bind to pattern recognition receptors, leading to a potent activation of inflammatory mediators, including inflammatory cytokines, chemokines, and cell adhesion molecules, thereby exacerbating the inflammatory injury once again. Therefore, numerous studies have demonstrated the importance of the innate immune response,[6,7] endothelial cell injury and regeneration[8,9] in determining cardiac function following myocardial injury.

Endothelial cells (ECs) play a critical role in myocardial ischemia-reperfusion injury, particularly in thrombosis, angiogenesis, and inflammatory responses.[10,11] Through paracrine signaling, ECs can regulate various pathophysiological processes, including the secretion of extracellular vesicles (EVs).[12]

EVs are a heterogeneous group of nanosized vesicles derived from cells that carry various nucleic acids and proteins to transfer information between cells. EVs have been associated with critical processes such as immune response, homeostasis, coagulation, inflammation, cancer progression, angiogenesis, and antigen presentation. Additionally, EVs can cross most biological barriers and have similar functions to their parent cells. Therefore, EVs have the potential to serve as biological mediators for the treatment of many diseases.[12,13] Several studies have demonstrated the important role of EVs in various diseases, including their potential as biomarkers, therapeutics, and drug delivery vehicles.[14–16] In the context of myocardial IR injury, EC-derived EVs have been shown to play a role in promoting angiogenesis, reducing apoptosis, and modulating inflammation.[17–20]

Recently, nasal administration has become an increasingly interesting way to administer drugs due to its convenience and noninvasiveness. As the nasal cavity is well vascularized, drugs can rapidly enter the systemic circulation after passing through the nasal epithelium.[21] However, there is limited research on whether nasally administered drugs can reach vital organ tissues such as the heart. Moreover, the dosing efficiency of its clinical application has remained a challenge.[22] It is good to know that low-molecular-weight gelator has shown great potential for intranasal delivery, and a two-component supramolecular hydrogel has been found to be suitable for nasal administration due to its appropriate rheological performance.[23,24] It would be intriguing to explore whether this hydrogel can effectively improve the

administration efficiency of EVs and whether the low-molecular-weight gelator +EVs can help improve cardiac function, endothelial barrier repair, and regulation of inflammatory responses after myocardial IR injury. Further research could shed light on the potential of this approach for treating cardiovascular disease.

Materials and Methods

Synthesis of L-Glutamine Dodecylamide

L-Glutamine dodecylamide was prepared following reported method.[25] Briefly, L-Boc-Gln-OH (247 mg, 1 mmol) was dissolved in dry DCM (15 mL) and stirred at 0°C for 5 minutes. Then EDC (330 mg, 1.8 mmol), DMAP (120 mg, 1 mmol) and dodecylamine (181 mg, 1 mmol) were added. The mixture was stirred under a nitrogen atmosphere for 2 h at 0°C and then at room temperature for 12 h. The reaction mixture was then washed with 2 M hydrochloric acid solution, water, 1 M NaOH and brine, 20 mL each. The organic layer was dried over sodium sulfate and the solvent was removed under reduced pressure. The crude product was purified by silica gel chromatography, using DCM/MeOH (35:1, v/v) as eluent to afford desired L-Boc-glutamine dodecylamide as a white solid (238 mg, 0.58 mmol, 58%) (Figure S1A). L-Boc-Gln dodecylamide (238 mg, 0.58 mmol) was added to a solution of 4 M HCl (8.7 mmol, 15 eq) in dioxane. After stirring at room temperature for 2 h, the solvent was removed under reduced pressure to yield a white solid. The solid was then deprotonated using NaOH (1 M) and extracted with DCM to give the free amine. The organic layer was dried over sodium sulfate and the solvent was removed under reduced pressure. The crude product was purified by silica gel chromatography, using DCM/MeOH (5:1, v/v) as eluent to afford desired L- glutamine dodecylamide as a white solid (71 mg, 0.23 mmol, 23%) (Figure S1B).

L-glutamine dodecylamide (3 mg), benzaldehyde (1 μL) was added to 0.8 mL of water, and the suspension was sonicated for 1 min and then left for 30 min to form the gel. Inversion test was used to check if a gel had formed. A small portion of gel was then transferred to a copper support, frozen by plunging into liquid nitrogen, and lyophilized for 12 hours. The dried sample with copper support was then mounted on an SEM stub using a carbon sticky tab, sputter-coated with a thin layer of gold, and then SEM images were recorded on an FEI Quanta 250 FEG microscope, operating at 20 kV.

EVs Isolation and Identification

MAECs were obtained from BeNa Culture Collection (BNCC359881). MAECs were cultured in DMEM (Thermo Fisher Scientific, 10,313–021) supplemented with 10% fetal bovine serum (Science Cell, 0025), 1% endothelial cell growth supplement (Science Cell, 1052) and 1% Penicillin/Streptomycin (Science Cell, 0503). The culture medium was refreshed regularly (2–3 times per week), and when the cell density reached 80%-90%, cells were either subcultured or cryopreserved. The subsequent experiments were performed using MAECs between passages 3 and 10. When the ECs reached 70% confluency, the culture medium was replaced with exosome-free serum (System Biosciences, EXO-FBS -50A-1) and cultured for 48h. EVs were extracted by standard differential centrifugation: the cell culture supernatant was centrifuged at 3000 g for 25 min and 10,000 g for 1 h to remove dead cells and debris. Then, the supernatant was centrifuged at 100,000 g for 3 hours, and the extracted EVs were re-suspended in PBS. The centrifugation was completed at 4 °C.

The structure of EVs was observed by transmission electron microscopy (JEM-1011 Japan), and the size of EVs was evaluated using the ZETA-VIEW (Particle Metrix). EVs were identified by marker proteins Alix (Santa Cruz, sc-53540), CD63 (Santa Cruz, sc-5275) and CD9 (Santa Cruz, sc-13118) through Western blots. The total protein concentration of EVs was determined using BCA assay (Thermo Scientific, 23225), and EVs were labeled with PKH67 (Sigma, PKH67GL) or DiD (Thermo Scientific, V22887) fluorescence. For EVs quantification, the protein concentration measured through BCA assay is strongly correlated with the particle count measured by NTA.[15] Therefore, we used BCA assay to determine the quantity of EVs in subsequent experiments.

L-glutamine dodecylamide (3 mg), benzaldehyde (1 μL) was added to 0.4 mL of water. Mix an appropriate amount of the above suspension with an equal amount of EVs solution (2 ug/μL), and the suspension was sonicated for 1 min to form the gel (EVs 1ug/μL). The hydrogel without EVs was formed using an equal amount of water.

EVs Release Analysis

The release of sEVs from the hydrogel was measured using the BCA protein assay kit, as described in the relevant study.[26] In brief, the hydrogel was immersed in PBS within a 24-well plate. At specific time intervals, surface supernatant was collected and fresh PBS was replenished. The released sEVs were quantified for protein content, providing the percentage of EVs released.

Animal Procedures

All animal procedures conformed to the Guide for Care and Use of Laboratory Animals published by the US National Institutes of Health (NIH; 8th edition, 2011) and were approved by and conducted according to the regulations and guidelines of the Institutional Ethics Committee of Nanjing Drum Tower Hospital (Approval No. 2023AE01020). This study used 8- to 10-week-old C57BL/6 male mice (purchased from the Model Animal Research Center of Nanjing University) and randomly allocated them to different experimental groups. The number of mice used for each experiment is indicated in the figure legends. All mice generated or purchased were housed in the Nanjing Drum Tower Hospital (Jiangsu, China) for at least 1 week before use.

Myocardial I/R model: the mice were first anesthetized with global anesthesia by isoflurane. During the operation, 1.5–2% isoflurane was used to maintain anesthesia. Small animal ventilator was used for assisted ventilation: 3 cm H_2O positive end-expiratory pressure, ventilation frequency 110 times/min, tidal volume 1.2 ~ 1.4 mL. Thoracotomy was performed at the 4th intercostal space to expose the heart and the left anterior descending coronary artery. We temporarily occluded the left anterior descending coronary artery using a 7–0 suture and released the suture after 60 minutes for reperfusion. We observed the electrocardiogram during the procedure and conducted echocardiography after the surgery to confirm the success of the modeling. In the sham operation group, all procedures and manipulations were identical to the modeling group, except that the left anterior descending coronary artery was not ligated, resulting in the absence of the cardiac ischemia-reperfusion process.

Mice were anesthetized with isoflurane and were given EVs hydrogel/solution intranasally, 2 μL each time, alternately into the left and right nostrils at intervals of 20s for total 20 μL (20 μg EVs) to allow sufficient retention of gel in nose and prevent dripping.

Echocardiography

For four consecutive weeks following myocardial ischemia-reperfusion injury in mice, two-dimensional short and long axis imaging was performed under light anesthesia to calculate LV functional parameters (Visual Sonics, Vevo 3100). LV end-systolic diameter (LVID;d), LV end-diastolic diameter (LVID;s), interventricular septal thickness (IVS), and LV posterior wall thickness (end-diastolic and end-systolic) were measured from at least three consecutive cardiac cycles on M-mode tracings. LV fractional shortening (FS %) was determined as [(LVID;d - LVID;s)/LVID;d] ×100. LV ejection fraction (EF) was calculated as: EF(%) = ((LV Vol;d - LV Vol;s)/LV Vol;d)×100. Here, LV Vol;d = ((7.0 / (2.4 + LVID;d)) × LVID;d^3) and LV Vol;s = ((7.0 / (2.4 + LVID;s)) × LVID;s^3).

Immunofluorescence Staining

Mouse samples were fixed in 4% paraformaldehyde for 2–3 h and washed with PBS for 20 min. The samples were then dehydrated overnight at 4 °C in PBS containing 30% sucrose, and then frozen sliced in Tissue-Tek OCT (SAKURA, 4583). Frozen sections (8μm) were incubated in a blocking buffer containing 10% goat serum, and incubated overnight at 4°C with primary antibody diluted in the blocking buffer. Sections were incubated with secondary antibody and DAPI (1μg/mL Sangon Biotech, E607303-0002) at room temperature in PBS for 2 h, then rinsed with PBS three times. The images were captured by THUNDER Imaging Systems. The antibodies used in this study include: anti-CD31 antibody (BD Pharmingen, 550274, 1:200), anti-CD68 antibody (Abcam, ab53444, 1:200), anti-vwf antibody (Abcam, ab287962, 1:200) and anti-albumin (Proteintech, 1645-1-AP), goat anti-rabbit IgG(H+L) Alexa Fluor 488 (Jackson immunoresearch, 112-545-144, 1:200), goat anti-rat IgG(H+L) Cy3 (Jackson immunoresearch, 112-165-167, 1:200).

Masson Trichrome, TTC and H&E Staining

The heart was collected at the appropriate time, embedded in paraffin, and cut into sections 5 μm thick. Sections were stained with Masson trichrome and H&E following the manufacturer's protocols.

Myocardial infarct size was detected by Evans blue dye and 2,3,5-triphenyl-2H-tetrazolium chloride (TTC, sigma, T8877) staining on day 3 after myocardial I/R injury. The area stained blue by Evans blue indicated the area not at risk, whereas the unstained tissues represented area-at-risk (AAR). AAR but viable tissue was stained red by TTC, while the infracted myocardium was not stained by any dye and appeared more pale than other areas. All quantitative statistics were performed using Image-Pro Plus software.

Flow Cytometry

The peripheral blood were incubated with red blood cell lysis buffer to lyse red blood cells. For the staining of certain cells, the cells were stained with conjugated antibodies (1 μL per 106 cells) for 30 min at 4 °C. The antibody used in this study were CD45 Monoclonal Antibody (PerCP-Cyanine5.5, eBioscience, 45-0451-82), CD11b Monoclonal Antibody (FITC, eBioscience, 11-0112-82), Ly-6C Monoclonal Antibody (APC, eBioscience, 17-5932-82 and PE, miltenyi biotec, 130-111-916) and Ly-6G Monoclonal Antibody (APC, eBioscience, 17-9668-82). The cells were then washed with PBS and resuspended in PBS containing 5% FBS for flow cytometric analysis (BD Accuri C6Plus). The FlowJo v10 software (Tree Star) was used to analyze the flow cytometric data.

Western Blot

Total protein was extracted from MACEs and EVs. Samples were lysed in cold lysis buffer containing protease inhibitors (KEYGEN BIOTECH, KGP603). 30μg of each protein sample was separated by SDS-PAGE gel (10%) and then transferred to a PVDF membrane (Millipore, Bedford, MA, USA). After blocking with 5% bovine serum albumin, blots were probed with a primary antibody (1:1000) and followed by a horseradish peroxidase-conjugated secondary antibody (1:4000). The following primary antibodies were used: Alix (Santa Cruz, sc-53540), CD63 (Santa Cruz, sc-5275), and CD9 (Santa Cruz, sc-13118). The secondary antibodies used were HRP-labeled Goat Anti-rabbit IgG(H+L) (Beyotime, A0208) and HRP-labeled Goat Anti-mouse IgG(H+L) (Beyotime, A0216). Enhanced chemiluminescence (ECL, thermofisher scientific) was used to detect protein levels on the blots.

ELISA

Inflammatory factors were detected by ELISA kits following the manufacturer's protocols (Multisciences EK282HS, EK206, EK201B).

Statistical Analyses

All data were determined from multiple individual biological samples and presented as mean values ± standard error of the mean. The "n" in the study represented the number of biological replicates, which is indicated in the figure legends. The GraphPad Prism 9 was used to perform the statistical analysis. The data were first subjected to a normality test, followed by analysis using unpaired Student's *t*-test or one-way ANOVA combined with Tukey's multiple comparisons test, as indicated in the figure legends. When comparing multiple groups, we conducted pairwise comparisons between each group. A p-value <0.05 indicated a statistically significant difference.

Results

Preparation of Hydrogel and Isolation of EVs

As low-molecular-weight gelators have shown great potential in drug delivery, we opted for a two-component gelation system as the exosome delivery vector. The system consists of a glutamine amine derivative and benzaldehyde, which, when mixed, undergo a reversible reaction to produce Schiff base and subsequently assemble into gels (Figure 1A). The hydrogels were characterized using scanning electron microscopy, as shown in Figure 1B.

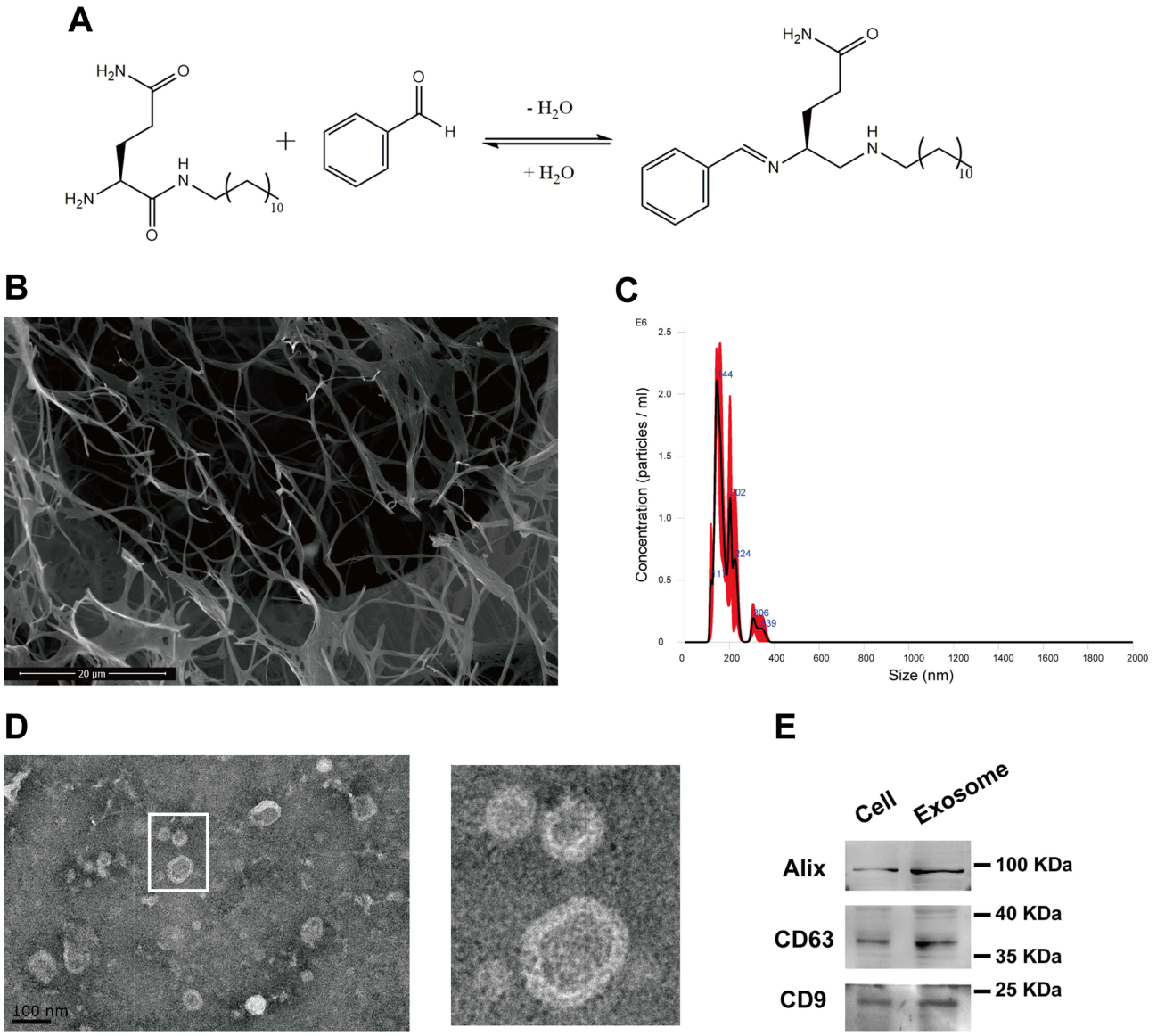

Figure 1 Preparation of Hydrogel and Extraction of EVs. (**A**) The gel is formed through the reaction of a glutamine amide derivative and benzaldehyde in water. (**B**) SEM image of the Gel sample. (**C**) Nanoparticle trafficking analyzed the diameters of the EVs. (**D**) TEM imaging of EVs derived from MAECs. (**E**) Representative images of WB. The surface markers include Alix, CD63, and CD9.

This gelator is an ideal vehicle for drug delivery applications, because Schiff bases do not persist in vivo for long periods due to hydrolysis and do not result in gelator deposition during repeated administration. The gelator will be decomposed into glutamine amide derivatives and benzaldehyde, which are generally regarded as safe.[27,28]

EVs were extracted from the culture supernatants of mouse aortic endothelial cells (MAECs) using a gradient centrifugation method. We characterized the phenotypic and morphological properties of the EVs. NTA analysis shows that the peak particle size of electric vehicles is at 144 nm (Figure 1C). And TEM imaging showed that the EVs had a double-layer membrane structure (Figure 1D). Additionally, we confirmed the presence of classical EV membrane proteins, including Alix, CD63, and CD9 (Figure 1E).

Intranasal Delivery of EVs with the Hydrogel Improved Administration Efficiency

To assess the advantages of hydrogels, we conducted in vivo and in vitro experiments. The release behavior of loaded EVs within the hydrogel is shown in Figure 2A, suggesting a sustained release of EVs within the hydrogel.

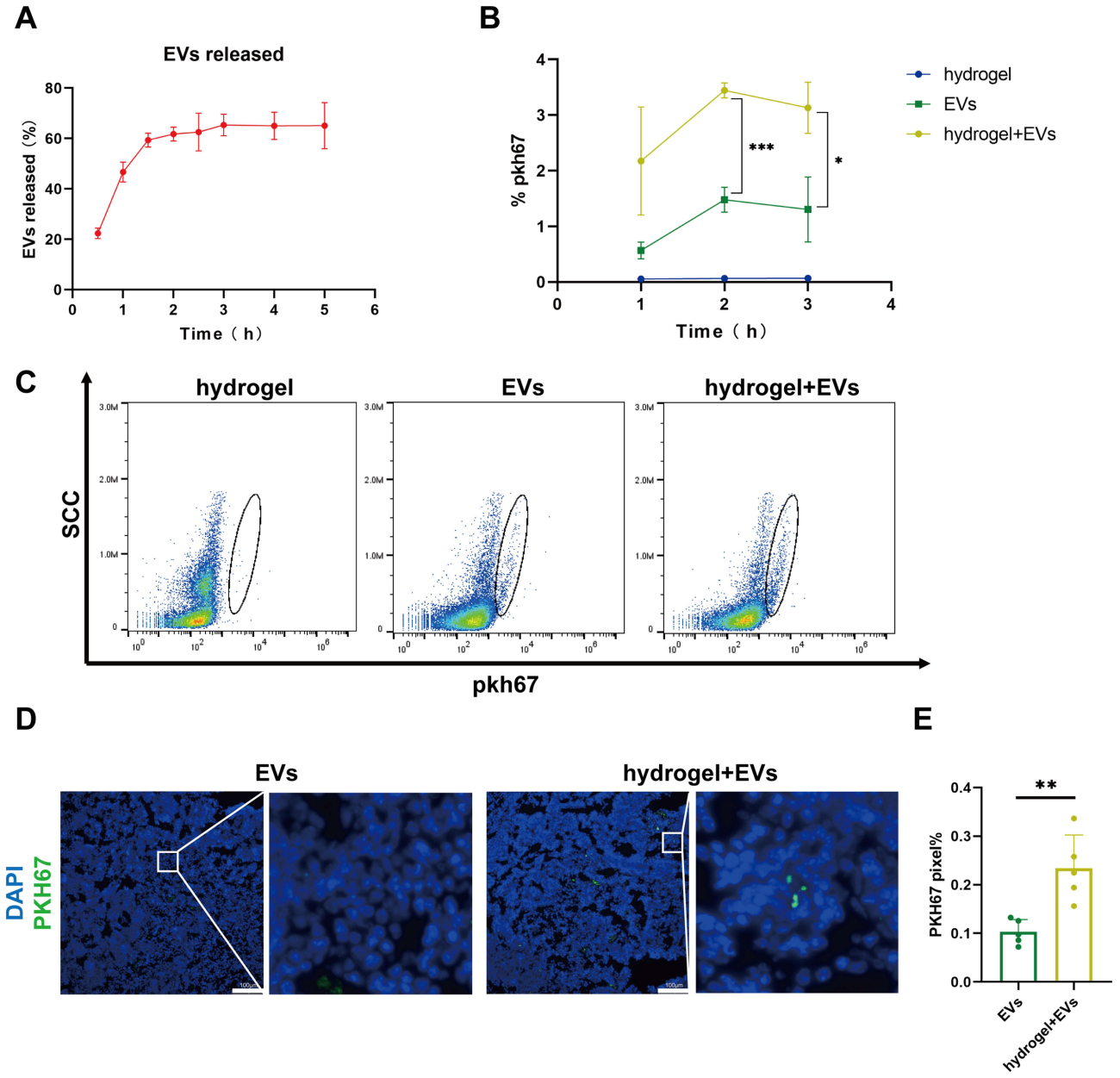

Figure 2 The hydrogel improved intranasal delivery efficiency. (**A**) Profile of sEVs released from the hydrogels (n=3). (**B** and **C**) Representative flow cytometry plots showing the PKH67^{+} cell in peripheral blood after intranasal administration and quantitative analysis of peripheral blood PKH67+ cells at different time points. (**D** and **E**) Representative cross-sections of spleen stained with DAPI (blue) and the quantification of PKH67^{+} pixel (n=5). (*P < 0.05, **P < 0.01, ***P < 0.001).

In vivo, we performed experiments with PKH67 or DiD-labeled EVs in C57BL/6 mice. Mice were intranasally administered, and the content of EVs within the mice was assessed at 1-, 2-, and 3-hours post-administration. Because EVs were labeled with PKH67 or DiD and the cells that captured EVs were also labeled with fluorescence. Flow cytometry analyses showed that intranasal delivery with the hydrogel made it easier to get EVs into circulation, and there were more fluorescent-labeled cells than mice administered with simple solution (Figure 2B and C). Moreover, the highest uptake of EVs was observed at the two-hour time point post-administration, consistent with the in vitro experimental findings. The hydrogel exhibits sustained release properties and can prolong the residence time of EVs in the nasal cavity, thereby enhancing their absorption.

We also detected the presence of EVs in various organs of mice, but almost no PKH67 signal was found in organs other than spleen by immunofluorescence (Figures 2D and S2). The result of fluorescence quantitative analysis was the same as

those of peripheral blood flow cytometry, intranasal delivery of EVs with the hydrogel formulation appeared to be more effective (Figure 2E). The mononuclear phagocyte system engulfs EVs, making it easier to detect their presence in organs rich in mononuclear macrophages such as the spleen, whereas targeting other organs may be more challenging.[29] So, we observed co-staining of CD68 (macrophage marker) and PKH67 in fluorescence staining (Figure S3A). In peripheral blood, we also identified fluorescent labeling within macrophages, indicating that macrophages are capable of internalizing EVs in the circulatory system (Figure S3B). These findings suggest that the hydrogel can improve the administration efficiency of EVs through intranasal delivery, but few EVs can infiltrate into various organs.

Intranasal Delivery of EVs Improved Cardiac Function in Myocardial I/R Injury Model

To investigate whether intranasal delivery of EVs improve myocardial I/R injury, mice were subjected to I/R injury surgery, followed by multiple intranasal deliveries of EVs either in a hydrogel formulation or a simple solution. The EVs were administered once a day for the first three days after I/R injury, and then twice a week (as shown in Figure 3A). The control group received an equal volume of hydrogel. Infarct size in mouse hearts was determined by Evan blue/TTC

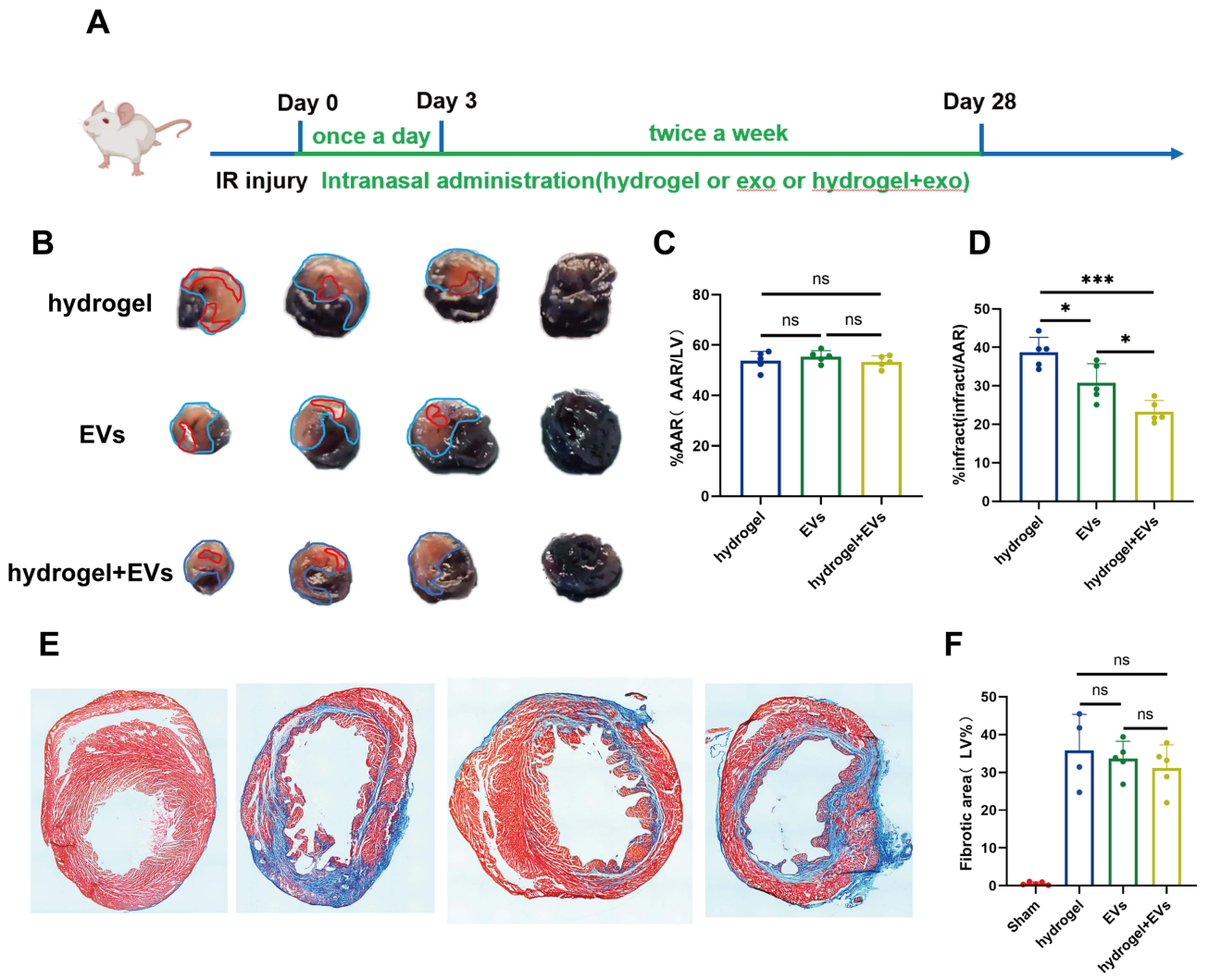

Figure 3 EVs with the hydrogel reduced the area of infarction after IR injury. (**A**) The mice underwent I/R injury surgery and were subsequently administered multiple intranasal doses of EVs, which were either in the form of a hydrogel formulation or a simple solution. (**B**) Representative images of Evans blue/TTC staining of mouse hearts taken 3 days later after myocardial IR injury (Area-at-risk; blue dotted line) and infarct size (red dotted line)). Quantitative analysis of AAR/left ventricle ratio (**C**) and infarct/AAR ratio (**D**) (n=5). (**E**) Representative images of masson trichrome staining of mouse hearts taken 28 days later after myocardial IR injury. (**F**) Quantitative analysis of fibrosis are/left ventricle ratio (n=5). (*P < 0.05, ***P < 0.001).

Abbreviation: ns, not significant.

staining on day 3 after myocardial I/R injury.[15] The area-of-risk (AAR) was similar among all groups, but the infarct area (infarct/AAR) was significantly lower in the EVs with hydrogel group than in the control group or the simple solution group (Figure 3B-D). After 28 days of myocardial IR injury, myocardial fibrosis in the mouse heart was evaluated using Masson trichrome staining. At this time, the repair of the mouse heart was essentially completed.[30] The area of cardiac collagen fibers did not differ significantly among all groups, indicating that intranasal delivery of EVs may not have a significant effect on cardiac fibrosis (Figure 3E and F).

Cardiac function was assessed in mice after I/R injury using echocardiography once a week. Compared to the sham group, cardiac function was significantly decreased after myocardial I/R injury. However, EVs with hydrogel significantly increased LVEF 14 days after myocardial IR injury (as shown in Figure 4A-H), indicating an improvement in cardiac function. Moreover, the improvement effect was better than that in the simple solution group. However, there was no significant difference in the ratio of dry lung weight to wet lung weight (WW/DW) and heart weight to tibia length (HW/TL) among all groups (Figure 4I and J). Overall, the results suggest that intranasal delivery of EVs with hydrogel can effectively improve cardiac function after myocardial I/R injury.

Intranasal Delivery of EVs Inhibited Inflammation in Myocardial I/R Injury Model

Repairing myocardial IR injury at the acute stage is often associated with a systemic inflammatory response, which can hinder the recovery of cardiac function. Fortunately, recent studies have shown that EVs can inhibit inflammatory responses, which makes them a promising therapeutic strategy for treating myocardial infarction.[17,31]

To investigate how EVs affect tissue repair, we measured the proportion of inflammatory cells in peripheral blood at the acute stage of myocardial infarction. Using flow cytometry, we found that EVs reduced the number of $Ly6C^{high}$ monocytes/macrophages ($CD45^{+}CD11b^{+}Ly6C^{high}$) (Figure 5A-C), which play a pro-inflammatory role.[32] Interestingly, we observed that the anti-inflammatory effect of EVs was even stronger when they were used in combination with a hydrogel.

We also found that treatment with EVs led to a significant decrease in the number of neutrophils ($CD45^{+}CD11b^{+}Ly6G^{+}$) in peripheral blood, and that the addition of the hydrogel further enhanced the therapeutic effect (Figure 5D and E). To confirm these findings, we measured the levels of inflammatory factors in peripheral blood using ELISA and performed immunofluorescence staining to reveal the difference in the number of macrophages (Figure 5H-J). The results of immunofluorescence staining were consistent with those obtained using flow cytometry, showing that EVs with the hydrogel had a stronger inhibitory effect on systemic inflammation and the homing of macrophages (Figure 5F and G). Our findings suggest that EVs, particularly when combined with a hydrogel, have potential as a therapeutic approach for treating myocardial IR injury by reducing the inflammatory response.

Intranasal Delivery of EVs Protected Endothelial Function in Myocardial I/R Injury Model

The EVs used were secreted by MAECs, and we were interested in exploring whether they had an effect on endothelial cells. To investigate this, we harvested mouse hearts on day 28 after myocardial IR injury and performed immunofluorescence staining using CD31 as a marker for microvascular density in the injured myocardium. The results of fluorescence quantitative analysis indicated that EVs in the hydrogel could contribute to angiogenesis after IR injury (Figure 6A and B).

We also investigated the effect of EVs on microthrombus formation, which is closely related to endothelial cells. Using vwf and thrombocyte as markers for thrombosis,[29,33,34] we observed a significant reduction in microthrombus formation in the injured area after intranasal treatment with EVs in combination with the hydrogel (Figure 6C-F). We used albumin fluorescence staining to assess the barrier function of the microcirculating endothelium.[34] Our results showed that albumin could cross the endothelial barrier after myocardial IR injury, but the albumin staining area significantly decreased after treatment with intranasal delivery of EVs in combination with the hydrogel (Figure 6G and H). These findings suggest that the hydrogel enhanced the protective effect of EVs on endothelial function. Taken together, our findings suggest that EVs derived from MAECs have a positive effect on endothelial function and angiogenesis after myocardial IR injury.

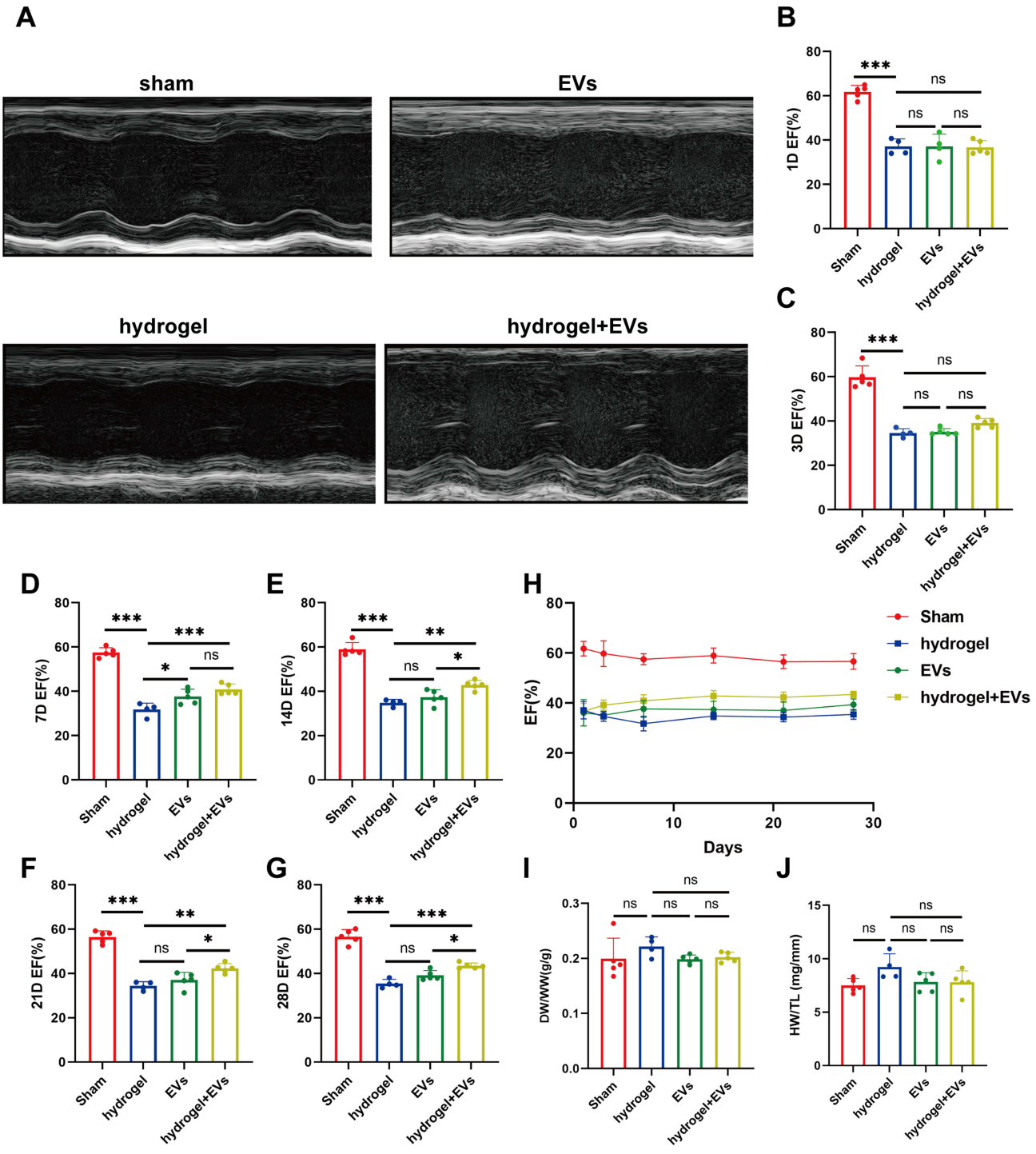

Figure 4 Intranasal delivery of EVs in the hydrogel improved cardiac function. (**A**) Left ventricular function was assessed by animal echocardiography (representative long-axis view of parasternal M-mode echocardiography). (**B-H**) Left ventricular ejection fraction (EF) at different time points. The ratio of DW/WW (**I**) and HW/TL (**J**) are shown. (n=4-5, *P < 0.05, **P < 0.01, ***P < 0.001).

Abbreviation: ns, not significant.

Finally, we assessed the biosafety of the hydrogel by performing H&E staining on major organs of mice without undergoing I/R injury surgery. Our results showed no significant pathological changes in major organs, including the heart, liver, spleen, kidney, and lung (Figure S4). Moreover, there was no significant difference in mortality among mice undergoing surgery for I/R injury. These results suggest that the hydrogel has no toxic side effects.

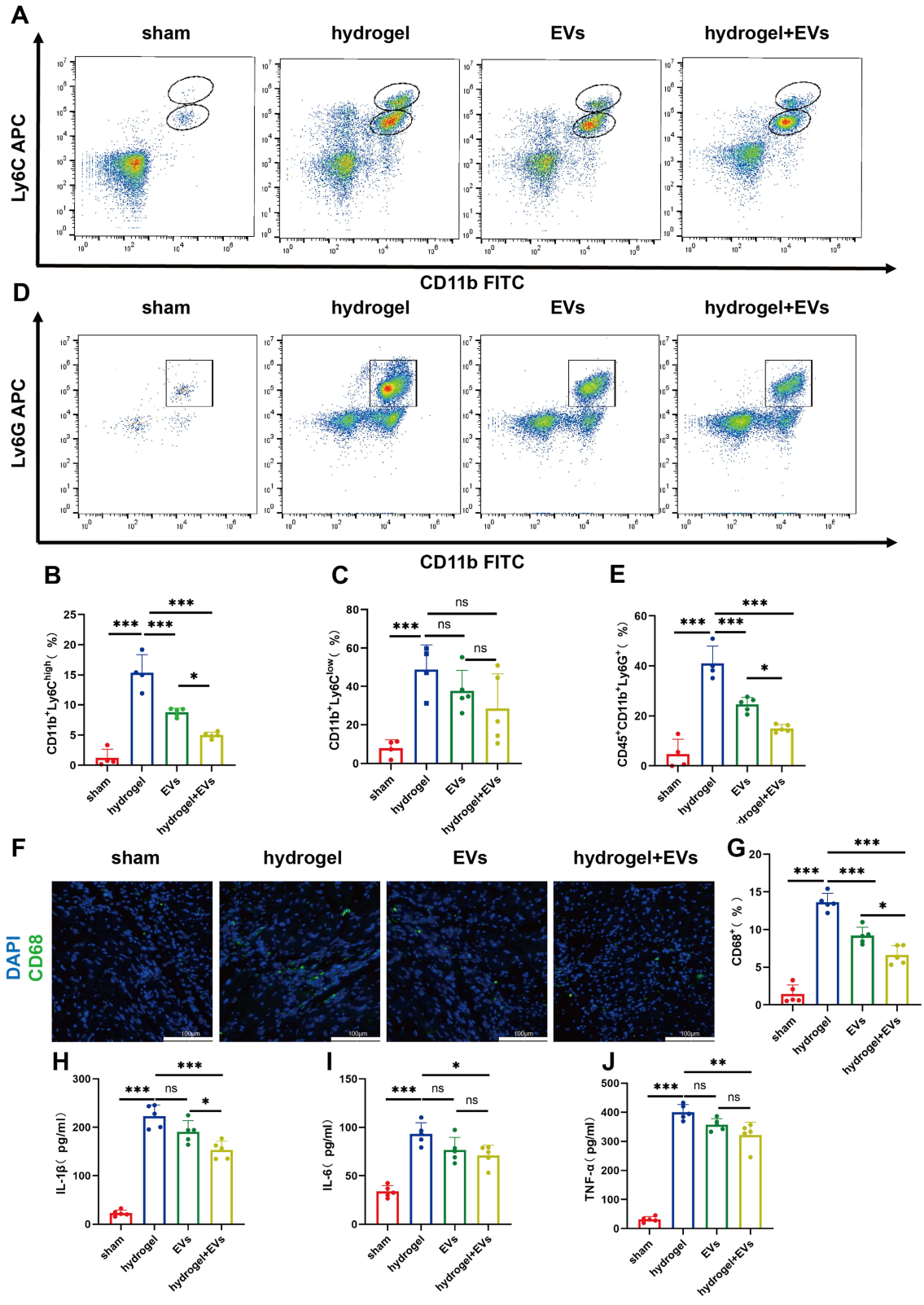

Figure 5 Intranasal delivery of EVs in the hydrogel inhibited inflammation. (**A**) Representative flow cytometry plots showing Ly6C^{high} monocyte and Ly6C^{low} monocytes/macrophages (CD45$^+$CD11b$^+$) in peripheral blood. and quantification of monocytes/macrophages (Ly6C$^{high\ or\ low}$) in peripheral blood. (n=5) (**B** and **C**). (**D**) Representative flow cytometry plots showing neutrophils (CD45$^+$CD11b$^+$Ly6G$^+$) in peripheral blood and quantification of neutrophils in peripheral blood. n=5. (**E**). (**F**) Representative images of ventricles staining CD68 (green) showing the infiltration status of macrophages and quantification of CD68$^+$ Cells. (n=5) (**G**). ELISA analysis of inflammatory factors IL-1 (**H**), IL-6 (**I**) and TNF-α (**J**) in peripheral blood. (n=5). (*P < 0.05, **P < 0.01, ***P < 0.001).

Abbreviation: ns, not significant.

https://doi.org/10.2147/IJN.S420301 DovePress

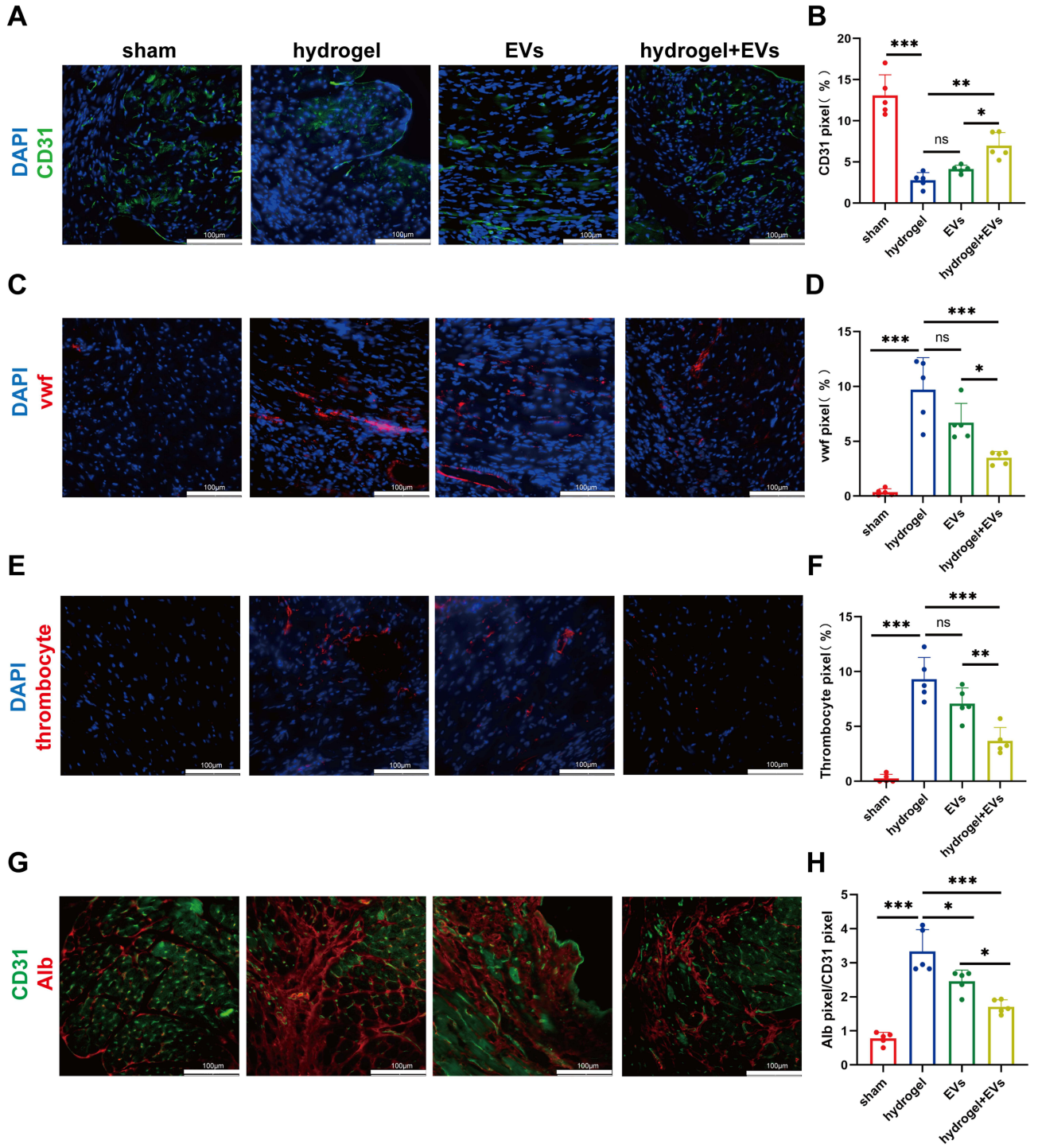

Figure 6 Intranasal delivery of EVs in the hydrogel protected endothelial function. (**A** and **B**) Representative images of ventricles staining CD31 (green) and DAPI (blue), along with quantitative results (n=5). (**C** and **D**) Representative images of ventricles staining vwf (red) and DAPI (blue), along with quantitative results (n=5). (**E** and **F**) Representative images of ventricles staining thrombocyte (red) and DAPI (blue), along with quantitative results (n=5). (**G** and **H**) Representative images of ventricles staining CD31 (green) and albumin (green), along with quantitative results (n=5). (*P < 0.05, **P < 0.01, ***P < 0.001).
Abbreviation: ns, not significant.

Discussion

This study aimed to investigate the effects of nasal administration of EVs in a hydrogel on myocardial IR injury. By combining EVs with a simple two-component supramolecular hydrogel, we were able to significantly increase the

efficiency of EVs absorption through the nasal cavity. Our findings demonstrated that the use of EVs combined with hydrogel led to a reduction in myocardial infarction area and an improvement in left ventricular systolic function in a mouse myocardial IR model compared to simple solution administration. Furthermore, we found that this beneficial effect was related to the inhibition of inflammatory response, the protection of endothelial cell function, and the promotion of capillary angiogenesis in the acute stage of cardiac injury. These results suggest that intranasal administration of EVs in hydrogel may represent a promising treatment option for the prevention and treatment of myocardial IR injury.

The intranasal route was chosen for drug delivery due to its noninvasive nature and convenience. The nasal mucosa contains abundant blood vessels and has high permeability, allowing for efficient drug absorption through this route.[35] In comparison to other delivery routes, intranasal administration offers advantages such as fast onset of action, high patient compliance, and avoidance of the first-pass effect of the liver.[22] Previous studies have demonstrated the effectiveness of intranasal administration of EVs in various diseases, particularly those affecting the nervous system.[36–38] However, the nasal cavity is covered by a mucous layer, and the mucociliary clearance system can quickly eliminate nasal drugs, leading to low absorption efficiency and potentially limiting the therapeutic effect compared to intravenous administration. To address this issue, some studies have explored methods to enhance the transmembrane and targeting capacity of EVs through EVs engineering,[39] which may improve the therapeutic efficacy. Additionally, it is worth exploring strategies to prolong the residence time of EVs in the nasal cavity to further improve their efficacy.

To improve the efficacy of intranasal administration and prolong the residence time of EVs in the nasal cavity, we utilized a simple two-component supramolecular hydrogel to combine with the EVs. The hydrogel has been previously described in detail and has been shown to possess suitable rheological properties for intranasal administration.[24,25] Softer gels are known to be more conducive to drug absorption.[40] The hydrogel tends to form a viscous liquid that can coat the nasal mucosa for a longer period of time, facilitating effective contact between the EVs and nasal epithelium. The in-situ self-assembly, soft rheological properties and sustained release capabilities of the gel were utilized to enhance the administration efficiency of EVs. As expected, our results demonstrated higher absorption efficiency for intranasal administration of EVs in the hydrogel. This suggests that the hydrogel has significant potential for use in the nasal delivery of EVs. This approach is particularly valuable for the treatment of EVs using non-intravenous administration. However, it should be noted that precisely because of the existence of the mononuclear phagocyte system,[29] the vast majority of EVs cannot infiltrate various organs, and their effects are still exerted by regulating peripheral inflammatory responses and thereby influencing the repair of cardiac injury.

The acute inflammatory response following cardiac injury is crucial for tissue repair after infarction. During this phase, cell death triggers innate immunity through endogenous danger-associated molecular patterns, which then bind to pattern recognition receptors and activate a cascade of inflammatory mediators, including cytokines, chemokines, and cell adhesion molecules.[4,6] In response to these signals, neutrophils and monocytes/macrophages become activated and recruited to the site of injury. Neutrophils are the first immune cells to infiltrate the damaged heart tissue.[41] Proinflammatory Ly6C^{high} monocytes/macrophages are also involved in the early inflammatory response through activation of the MCP-1/CCR2 axis.[42]

Tissue repair of the heart following myocardial infarction and revascularization requires timely induction of inflammation to remove necrotic cells and tissues, but it is also crucial to halt the inflammatory response in a timely manner. Lower levels of pro-inflammatory cytokines have been shown to reduce inflammatory cell infiltration, myocardial infarction area, and poor ventricular remodeling in numerous studies.[43,44] Overactivation of Ly6C^{high} monocytes/macrophages and neutrophils can also have a negative impact on heart tissue repair.[15,31,45] In this study, we observed a significant decrease in pro-inflammatory factors (IL-1, IL-6, and TNF-α) after EVs in hydrogel treatment, as well as a decrease in neutrophils and Ly6c^{high} monocytes/macrophages in peripheral blood, consistent with previous research.[17,46] These results are also consistent with the observed reduction in myocardial infarction area and improvement in cardiac function in mice. Therefore, intranasal administration of EVs may have a positive role in reducing inflammation, protecting the heart, and decreasing myocardial infarction area.

ECs play an important role in reducing inflammation, preventing thrombosis, and promoting angiogenesis.[47] However, prolonged ischemia or reperfusion can lead to EC damage, microthrombus formation, and microvascular

destruction, which can further exacerbate cardiac injury.[48] In our study, we found that endothelium-derived EVs in mouse aorta seemed to ameliorate some of the damage. Our results show that after treatment with EVs in hydrogels, microthrombus formation is reduced, angiogenesis is increased, and the endothelial barrier is more intact because of a reduction in systemic inflammation, which may contribute to the recovery of cardiac function.

There are still many limitations to this study. After entering the peripheral circulation, EVs are rapidly engulfed by the mononuclear phagocyte system, making it difficult for them to infiltrate cardiac tissue and limiting their further action. Therefore, how to achieve immune escape will be the main focus of our future research. Additionally, there are many active substances present in EVs, and their specific mechanisms of action require further exploration.

Conclusion

Our study demonstrated that the intranasal administration of MAECs-derived EVs combined with a two-component supramolecular hydrogel is an effective method for delivering EVs into the peripheral blood. This approach was shown to inhibit the inflammatory response and protect endothelial cells in mice with myocardial ischemia-reperfusion injury, resulting in improved cardiac function and reduced infarct size. Our findings suggest that intranasal administration of EVs in a hydrogel could be a promising strategy for the treatment of cardiac injury.

Abbreviations

IR, Ischemia-reperfusion; ECs, Endothelial cells; EVs, Extracellular vesicles; MAECs, Mouse aortic endothelial cells; AAR, Area of risk; DW/WW, The ratio of dry lung weight to wet lung weight; HW/TL, Heart weight to tibia length.

Data Sharing Statement

The detailed experimental methods and additional figures can be found in the Supplementary Materials. The data that support the findings of this study are available from the corresponding author upon reasonable request.

Ethics Approval and Informed Consent

All animal procedures conformed to the Guide for Care and Use of Laboratory Animals published by the US National Institutes of Health (NIH; 8th edition, 2011) and were approved by and conducted according to the regulations and guidelines of the Institutional Ethics Committee of Nanjing Drum Tower Hospital (Approval No. 2023AE01020).

Author Contributions

All authors have made significant contributions to the work reported, including conception, study design, execution, data acquisition, analysis and interpretation, as well as manuscript drafting, revision, and critical review. All authors have provided final approval of the submitted version for publication and have agreed to the journal to which the article has been submitted, with full accountability for all aspects of the work.

Funding

This work was supported by grants from the National Natural Science Foundation of China (21708019, 82200380, 82070366), China Postdoctoral Science Foundation (2022M711588) and Natural Science Foundation of Jiangsu Province (BK20220174).

Disclosure

The authors report no conflicts of interest in this work.

References

1. Yeh RW, Sidney S, Chandra M, Sorel M, Selby JV, Go AS. Population trends in the incidence and outcomes of acute myocardial infarction. *N Engl J Med*. 2010;362(23):2155–2165. doi:10.1056/NEJMoa0908610
2. Davidson SM, Ferdinandy P, Andreadou I, et al. Multitarget Strategies to Reduce Myocardial Ischemia/Reperfusion Injury: JACC Review Topic of the Week. *J Am Coll Cardiol*. 2019;73(1):89–99. doi:10.1016/j.jacc.2018.09.086

3. Neri M, Riezzo I, Pascale N, Pomara C, Turillazzi E. Ischemia/Reperfusion Injury following Acute Myocardial Infarction: a Critical Issue for Clinicians and Forensic Pathologists. *Mediators Inflamm*. 2017;2017:7018393. doi:10.1155/2017/7018393
4. Prabhu SD, Frangogiannis NG. The Biological Basis for Cardiac Repair After Myocardial Infarction: from Inflammation to Fibrosis. *Circ Res*. 2016;119(1):91–112. doi:10.1161/CIRCRESAHA.116.303577
5. Kain V, Prabhu SD and Halade GV. Inflammation revisited: inflammation versus resolution of inflammation following myocardial infarction. *Basic Res Cardiol*. 2014;109(6):444. doi: 10.1007/s00395-014-0444-7
6. Timmers L, Pasterkamp G, de Hoog VC, Arslan F, Appelman Y, de Kleijn DP. The innate immune response in reperfused myocardium. *Cardiovasc Res*. 2012;94(2):276–283. doi:10.1093/cvr/cvs018
7. Ong SB, Hernandez-Resendiz S, Crespo-Avilan GE, et al. Inflammation following acute myocardial infarction: multiple players, dynamic roles, and novel therapeutic opportunities. *Pharmacol Ther*. 2018;186:73–87. doi:10.1016/j.pharmthera.2018.01.001
8. Wu X, Reboll MR, Korf-Klingebiel M, Wollert KC. Angiogenesis after acute myocardial infarction. *Cardiovasc Res*. 2021;117(5):1257–1273. doi:10.1093/cvr/cvaa287
9. Tombor LS, John D, Glaser SF, et al. Single cell sequencing reveals endothelial plasticity with transient mesenchymal activation after myocardial infarction. *Nat Commun*. 2021;12(1):681. doi:10.1038/s41467-021-20905-1
10. Godo S, Shimokawa H. Endothelial Functions. *Arterioscler Thromb Vasc Biol*. 2017;37(9):e108–e114. doi:10.1161/ATVBAHA.117.309813
11. Vancheri F, Longo G, Vancheri S, Henein M. Coronary Microvascular Dysfunction. *J Clin Med*. 2020;9(9):2880. doi:10.3390/jcm9092880
12. Hosseinkhani B, Kuypers S, van den Akker NMS, Molin DGM, Michiels L. Extracellular Vesicles Work as a Functional Inflammatory Mediator Between Vascular Endothelial Cells and Immune Cells. *Front Immunol*. 2018;9:1789. doi:10.3389/fimmu.2018.01789
13. Li M, Li S, Du C, et al. Exosomes from different cells: characteristics, modifications, and therapeutic applications. *Eur J Med Chem*. 2020;207:112784. doi:10.1016/j.ejmech.2020.112784
14. Hoshino A, Kim HS, Bojmar L, et al. Extracellular Vesicle and Particle Biomarkers Define Multiple Human Cancers. *Cell*. 2020;182(4):1044–1061 e18. doi:10.1016/j.cell.2020.07.009
15. Zhao J, Li X, Hu J, et al. Mesenchymal stromal cell-derived exosomes attenuate myocardial ischaemia-reperfusion injury through miR-182-regulated macrophage polarization. *Cardiovasc Res*. 2019;115(7):1205–1216. doi:10.1093/cvr/cvz040
16. Sadeghi S, Tehrani FR, Tahmasebi S, Shafiee A, Hashemi SM. Exosome engineering in cell therapy and drug delivery. *Inflammopharmacology*. 2023;31(1):145–169. doi:10.1007/s10787-022-01115-7
17. Njock MS, Cheng HS, Dang LT, et al. Endothelial cells suppress monocyte activation through secretion of extracellular vesicles containing antiinflammatory microRNAs. *Blood*. 2015;125(20):3202–3212. doi:10.1182/blood-2014-11-611046
18. Paone S, Baxter AA, Hulett MD, Poon IKH. Endothelial cell apoptosis and the role of endothelial cell-derived extracellular vesicles in the progression of atherosclerosis. *Cell Mol Life Sci*. 2019;76(6):1093–1106. doi:10.1007/s00018-018-2983-9
19. Togliatto G, Dentelli P, Rosso A, et al. PDGF-BB Carried by Endothelial Cell-Derived Extracellular Vesicles Reduces Vascular Smooth Muscle Cell Apoptosis in Diabetes. *Diabetes*. 2018;67(4):704–716. doi:10.2337/db17-0371
20. Todorova D, Simoncini S, Lacroix R, Sabatier F, Dignat-George F. Extracellular Vesicles in Angiogenesis. *Circ Res*. 2017;120(10):1658–1673. doi:10.1161/CIRCRESAHA.117.309681
21. Herman S, Fishel I, Offen D. Intranasal delivery of mesenchymal stem cells-derived extracellular vesicles for the treatment of neurological diseases. *Stem Cells*. 2021, 39(12):1589–1600. doi:10.1002/stem.3456
22. Tai J, Han M, Lee D, Park IH, Lee SH, Kim TH. Different Methods and Formulations of Drugs and Vaccines for Nasal Administration. *Pharmaceutics*. 2022;14(5):1073. doi:10.3390/pharmaceutics14051073
23. Du X, Zhou J, Shi J, Xu B. Supramolecular Hydrogelators and Hydrogels: from Soft Matter to Molecular Biomaterials. *Chem Rev*. 2015;115 (24):13165–13307. doi:10.1021/acs.chemrev.5b00299
24. Wang JT, Rodrigo AC, Patterson AK, et al. Enhanced Delivery of Neuroactive Drugs via Nasal Delivery with a Self-Healing Supramolecular Gel. *Adv Sci*. 2021;8(14):e2101058. doi:10.1002/advs.202101058
25. Hawkins K, Patterson AK, Clarke PA, Smith DK. Catalytic Gels for a Prebiotically Relevant Asymmetric Aldol Reaction in Water: from Organocatalyst Design to Hydrogel Discovery and Back Again. *J Am Chem Soc*. 2020;142(9):4379–4389. doi:10.1021/jacs.9b13156
26. Hu H, Dong L, Bu Z, Shen Y, Liu Z. miR-23a-3p-abundant small extracellular vesicles released from Gelma/nanoclay hydrogel for cartilage regeneration. *J Extracell Vesicles*. 2020;9(1):1778883.
27. Laham S, Broxup B, Robinet M, Potvin M, Schrader K. Subacute inhalation toxicity of benzaldehyde in the Sprague-Dawley rat. *Am Ind Hyg Assoc J*. 1991;52(12):503–510. doi:10.1080/15298669191365126
28. Andersen A. Final report on the safety assessment of benzaldehyde. *Int J Toxicol*. 2006;25(Suppl 1):11–27. doi:10.1080/10915810600716612
29. Wan Z, Zhao L, Lu F, et al. Mononuclear phagocyte system blockade improves therapeutic exosome delivery to the myocardium. *Theranostics*. 2020;10(1):218–230. doi:10.7150/thno.38198
30. Humeres C, Frangogiannis NG. Fibroblasts in the Infarcted, Remodeling, and Failing Heart. *JACC Basic Translational Sci*. 2019;4(3):449–467. doi:10.1016/j.jacbts.2019.02.006
31. Qiao S, Zhang W, Yin Y, et al. Extracellular vesicles derived from Kruppel-Like Factor 2-overexpressing endothelial cells attenuate myocardial ischemia-reperfusion injury by preventing Ly6C(high) monocyte recruitment. *Theranostics*. 2020;10(25):11562–11579. doi:10.7150/thno.45459
32. Leuschner F, Panizzi P, Chico-Calero I, et al. Angiotensin-converting enzyme inhibition prevents the release of monocytes from their splenic reservoir in mice with myocardial infarction. *Circ Res*. 2010;107(11):1364–1373. doi:10.1161/CIRCRESAHA.110.227454
33. Shahidi M. Thrombosis and von Willebrand Factor. *Adv Exp Med Biol*. 2017;906:285–306. doi:10.1007/5584_2016_122
34. Zhang X, Gong P, Zhao Y, et al. Endothelial caveolin-1 regulates cerebral thrombo-inflammation in acute ischemia/reperfusion injury. *EBioMedicine*. 2022;84:104275. doi:10.1016/j.ebiom.2022.104275
35. Grassin-Delyle S, Buenestado A, Naline E, et al. Intranasal drug delivery: an efficient and non-invasive route for systemic administration: focus on opioids. *Pharmacol Ther Jun*. 2012;134(3):366–379. doi:10.1016/j.pharmthera.2012.03.003
36. Cone AS, Yuan X, Sun L, et al. Mesenchymal stem cell-derived extracellular vesicles ameliorate Alzheimer's disease-like phenotypes in a preclinical mouse model. *Theranostics*. 2021;11(17):8129–8142. doi:10.7150/thno.62069

37. Narbute K, Pilipenko V, Pupure J, et al. Intranasal Administration of Extracellular Vesicles Derived from Human Teeth Stem Cells Improves Motor Symptoms and Normalizes Tyrosine Hydroxylase Expression in the Substantia Nigra and Striatum of the 6-Hydroxydopamine-Treated Rats. *Stem Cells Transl Med*. 2019;8(5):490–499. doi:10.1002/sctm.18-0162
38. Losurdo M, Pedrazzoli M, D'Agostino C, et al. Intranasal delivery of mesenchymal stem cell-derived extracellular vesicles exerts immunomodulatory and neuroprotective effects in a 3xTg model of Alzheimer's disease. *Stem Cells Transl Med*. 2020;9(9):1068–1084. doi:10.1002/sctm.19-0327
39. Peng H, Li Y, Ji W, et al. Intranasal Administration of Self-Oriented Nanocarriers Based on Therapeutic Exosomes for Synergistic Treatment of Parkinson's Disease. *ACS Nano*. 2022;16(1):869–884. doi:10.1021/acsnano.1c08473
40. Nguyen DV, Li F, Li H, et al. Drug permeation through skin is inversely correlated with carrier gel rigidity. *Mol Pharm*. 2015;12(2):444–452. doi:10.1021/mp500542a
41. Frangogiannis NG. Regulation of the inflammatory response in cardiac repair. *Circ Res*. 2012;110(1):159–173. doi:10.1161/CIRCRESAHA.111.243162
42. Dewald O, Zymek P, Winkelmann K, et al. CCL2/Monocyte Chemoattractant Protein-1 regulates inflammatory responses critical to healing myocardial infarcts. *Circ Res*. 2005;96(8):881–889. doi:10.1161/01.RES.0000163017.13772.3a
43. Bujak M, Dobaczewski M, Chatila K, et al. Interleukin-1 receptor type I signaling critically regulates infarct healing and cardiac remodeling. *Am J Pathol*. 2008;173(1):57–67. doi:10.2353/ajpath.2008.070974
44. Hilfiker-Kleiner D, Shukla P, Klein G, et al. Continuous glycoprotein-130-mediated signal transducer and activator of transcription-3 activation promotes inflammation, left ventricular rupture, and adverse outcome in subacute myocardial infarction. *Circulation*. 2010;122(2):145–155. doi:10.1161/CIRCULATIONAHA.109.933127
45. Wan Q, Xu C, Zhu L, et al. Targeting PDE4B (Phosphodiesterase-4 Subtype B) for Cardioprotection in Acute Myocardial Infarction via Neutrophils and Microcirculation. *Circ Res*. 2022;131(5):442–455. doi:10.1161/CIRCRESAHA.122.321365
46. Cantaluppi V, Gatti S, Medica D, et al. Microvesicles derived from endothelial progenitor cells protect the kidney from ischemia-reperfusion injury by microRNA-dependent reprogramming of resident renal cells. *Kidney Int*. 2012;82(4):412–427. doi:10.1038/ki.2012.105
47. Deanfield JE, Halcox JP, Rabelink TJ. Endothelial function and dysfunction: testing and clinical relevance. *Circulation*. 2007;115(10):1285–1295. doi:10.1161/CIRCULATIONAHA.106.652859
48. Dube KN, Thomas TM, Munshaw S, Rohling M, Riley PR, Smart N. Recapitulation of developmental mechanisms to revascularize the ischemic heart. *JCI Insight*. 2017;2(22). doi:10.1172/jci.insight.96800